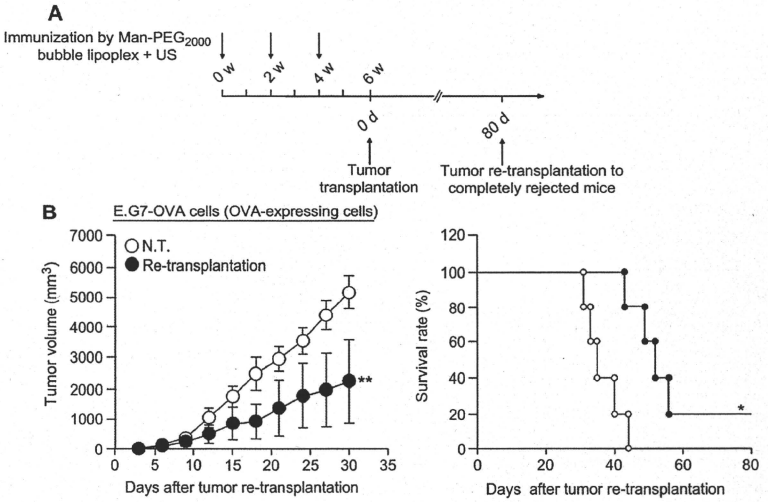

Fig. 11. Maintaining of Anti-tumor effects by DNA vaccination using Man-PEG_{2000} bubble lipoplexes and US exposure. At 80 days after first transplantation of E.G7-OVA cells to immunized mice three times by Man-PEG_{2000} bubble lipoplexes and US exposure, E.G7-OVA cells (1×10^6 cells) were re-transplanted subcutaneously into the back of mice which the first-transplanted tumors were completely rejected ($n = 5$). The tumor volume was evaluated (each value represents the mean ± SD) and the survival was monitored up to 80 days after the tumor re-transplantation. $^*p < 0.05$; $^{**}p < 0.01$, compared with the corresponding group of N.T. N.T., non-treatment.

various types of nucleic acids, such as NF-κB decoy [48], ICAM-1 antisense oligonucleotides [49], with low doses of nucleic acids. Moreover, organ-specific gene expression was observed in US-exposed organ by exposing US to the organ directly after intravenous administration of Man-PEG_{2000} bubble lipoplexes (Supplementary Fig. 5); therefore the beforehand knockdown of inflammatory factors such as NF-κB or ICAM-1 by Man-PEG_{2000} bubble lipoplexes and US exposure might be available for the prevention of ischemia reperfusion injury, a major problem in living donor liver transplantation.

5. Conclusion

In this study, we developed the gene transfection method using Man-PEG_{2000} bubble lipoplexes and US exposure. This transfection method enabled APC-selective and efficient gene expression, and moreover, effective anti-tumor effects was obtained by applying this method to DNA vaccine therapy against cancer. This method could be widely used in a variety of targeted cell-selective and efficient gene transfection methods by substituting mannose with various ligands reported previously [2–6]. In addition, in this gene transfection method, pDNA can directly introduce the nucleic acids into the cells through the transient pores created by US-responsive degradation of bubble lipoplexes, therefore this method could apply to many ligands which are not taken up via endocytosis. These findings make a valuable contribution to overcome the poor introducing efficiency into cytoplasm which is a major obstacle for gene delivery by non-viral vectors, and show that this method is an effective method for in-vivo gene delivery.

Acknowledgements

This work was supported in part by Grant-in-Aid for Scientific Research from the Ministry of Education, Culture, Sports, Science and Technology of Japan, and by Health and Labour Sciences Research Grants for Research on Noninvasive and Minimally Invasive Medical Devices from the Ministry of Health, Labour and Welfare of Japan, and by the Programs for Promotion of Fundamental Studies in Health Sciences of the National Institute of Biomedical Innovation (NIBIO), and by the Japan Society for the Promotion of Sciences (JSPS) through a JSPS Research Fellowship for Young Scientists.

Appendix. Supplementary data

Supplementary data associated with this article can be found, in the online version, at doi:10.1016/j.biomaterials.2010.06.058.

References

[1] Kawakami S, Sato A, Nishikawa M, Yamashita F, Hashida M. Mannose receptor-mediated gene transfer into macrophages using novel mannosylated cationic liposomes. Gene Ther 2000;7:292–9.
[2] Schiffelers RM, Koning GA, ten Hagen TL, Fens MH, Schraa AJ, Janssen AP, et al. Anti-tumor efficacy of tumor vasculature-targeted liposomal doxorubicin. J Control Release 2003;91:115–22.
[3] Torchilin VP, Levchenko TS, Rammohan R, Volodina N, Papahadjopoulos-Sternberg B, D'Souza GG. Cell transfection in vitro and in vivo with nontoxic TAT peptide–liposome–DNA complexes. Proc Natl Acad Sci U S A 2003;100:1972–7.
[4] Kirpotin DB, Drummond DC, Shao Y, Shalaby MR, Hong K, Nielsen UB, et al. Antibody targeting of long-circulating lipidic nanoparticles does not increase tumor localization but does increase internalization in animal models. Cancer Res 2006;66:6732–40.

[5] Goldstein D, Gofrit O, Nyska A, Benita S. Anti-HER2 cationic immunoemulsion as a potential targeted drug delivery system for the treatment of prostate cancer. Cancer Res 2007;67:269–75.
[6] Oba M, Aoyagi K, Miyata K, Matsumoto Y, Itaka K, Nishiyama N, et al. Polyplex micelles with cyclic RGD peptide ligands and disulfide cross-links directing to the enhanced transfection via controlled intracellular trafficking. Mol Pharmacol 2008;5:1080–92.
[7] Sheng KC, Kalkanidis M, Pouniotis DS, Esparon S, Tang CK, Apostolopoulos V, et al. Delivery of antigen using a novel mannosylated dendrimer potentiates immunogenicity in vitro and in vivo. Eur J Immunol 2008;38:424–36.
[8] Satkauskas S, Bureau MF, Puc M, Mahfoudi A, Scherman D, Miklavcic D, et al. Mechanisms of in vivo DNA electrotransfer: respective contributions of cell electropermeabilization and DNA electrophoresis. Mol Ther 2002;5:133–40.
[9] Mukai H, Kawakami S, Kamiya Y, Ma F, Takahashi H, Satake K, et al. Pressure-mediated transfection of murine spleen and liver. Hum Gene Ther 2009;20:1157–67.
[10] Nishikawa M, Nakayama A, Takahashi Y, Fukuhara Y, Takakura Y. Reactivation of silenced transgene expression in mouse liver by rapid, large-volume injection of isotonic solution. Hum Gene Ther 2008;19:1009–20.
[11] Hernot S, Klibanov AL. Microbubbles in ultrasound-triggered drug and gene delivery. Adv Drug Deliv Rev 2008;60:1153–66.
[12] Suzuki R, Takizawa T, Negishi Y, Utoguchi N, Sawamura K, Tanaka K, et al. Tumor specific ultrasound enhanced gene transfer in vivo with novel liposomal bubbles. J Control Release 2008;125:137–44.
[13] Negishi Y, Endo Y, Fukuyama T, Suzuki R, Takizawa T, Omata D, et al. Delivery of siRNA into the cytoplasm by liposomal bubbles and ultrasound. J Control Release 2008;132:124–30.
[14] Lentacker I, Geers B, Demeester J, De Smedt SC, Sanders NN. Design and evaluation of doxorubicin-containing microbubbles for ultrasound-triggered doxorubicin delivery: cytotoxicity and mechanisms involved. Mol Ther 2010;18:101–8.
[15] Liu Y, Miyoshi H, Nakamura M. Encapsulated ultrasound microbubbles: therapeutic application in drug/gene delivery. J Control Release 2006;114:89–99.
[16] Un K, Kawakami S, Suzuki R, Maruyama K, Yamashita F, Hashida M. Enhanced transfection efficiency into macrophages and dendritic cells by the combination method using mannosylated lipoplexes and bubble liposomes with ultrasound exposure. Hum Gene Ther 2010;21:65–74.
[17] Kawabata K, Takakura Y, Hashida M. The fate of plasmid DNA after intravenous injection in mice: involvement of scavenger receptors in its hepatic uptake. Pharm Res 1995;12:825–30.
[18] Potter NS, Harding CV. Neutrophils process exogenous bacteria via an alternate class I MHC processing pathway for presentation of peptides to T lymphocytes. J Immunol 2001;167:2538–46.
[19] Hattori Y, Suzuki S, Kawakami S, Yamashita F, Hashida M. The role of dioleoylphosphatidylethanolamine (DOPE) in targeted gene delivery with mannosylated cationic liposomes via intravenous route. J Control Release 2005;108:484–95.
[20] Hattori Y, Kawakami S, Lu Y, Nakamura K, Yamashita F, Hashida M. Enhanced DNA vaccine potency by mannosylated lipoplex after intraperitoneal administration. J Gene Med 2006;8:824–34.
[21] Lee YC. 2-Imino-2-methoxyethyl 1-thioglycosides: new reagents for attaching sugars to proteins. Biochemistry 1976;15:3956–63.
[22] Wang LH, Rothberg KG, Anderson RG. Mis-assembly of clathrin lattices on endosomes reveals a regulatory switch for coated pit formation. J Cell Biol 1993;123:1107–17.
[23] Akiyama T, Ishida J, Nakagawa S, Ogawara H, Watanabe S, Itoh N, et al. Genistein, a specific inhibitor of tyrosine-specific protein kinases. J Biol Chem 1987;262:5592–5.
[24] West MA, Bretscher MS, Watts C. Distinct endocytotic pathways in epidermal growth factor-stimulated human carcinoma A431 cells. J Cell Biol 1989;109:2731–9.
[25] Hattori Y, Kawakami S, Nakamura K, Yamashita F, Hashida M. Efficient gene transfer into macrophages and dendritic cells by in vivo gene delivery with mannosylated lipoplex via the intraperitoneal route. J Pharmacol Exp Ther 2006;318:828–34.
[26] Rigby PWJ, Dieckmann M, Rhodes C, Berg P. Labeling deoxyribonucleic acid to high specific activity in vitro by nick translation with DNA polymerase I. J Mol Biol 1977;113:237–51.
[27] Kawakami S, Wong J, Sato A, Hattori Y, Yamashita F, Hashida M. Biodistribution characteristics of mannosylated, fucosylated, and galactosylated liposomes in mice. Biochim Biophys Acta 2000;1524:258–65.
[28] Taylor PR, Gordon S, Martinez-Pomares L. The mannose receptor: linking homeostasis and immunity through sugar recognition. Trends Immunol 2005;26:104–10.
[29] Tacken PJ, de Vries IJ, Torensma R, Figdor CG. Dendritic-cell immunotherapy: from ex vivo loading to in vivo targeting. Nat Rev Immunol 2007;7:790–802.
[30] Kurts C. CD11c: not merely a murine DC marker, but also a useful vaccination target. Eur J Immunol 2008;38:2072–5.
[31] Steinman RM, Banchereau J. Taking dendritic cells into medicine. Nature 2007;449:419–26.
[32] Hume DA. Macrophages as APC and the dendritic cell myth. J Immunol 2008;181:5829–35.
[33] Liu K, Waskow C, Liu X, Yao K, Hoh J, Nussenzweig M. Origin of dendritic cells in peripheral lymphoid organs of mice. Nat Immunol 2007;8:578–83.
[34] Abe Y, Kuroda Y, Kuboki N, Matsushita M, Yokoyama N, Kojima N. Contribution of complement component C3 and complement receptor type 3 to carbohydrate-dependent uptake of oligomannose-coated liposomes by peritoneal macrophages. J Biochem 2008;144:563–70.
[35] Sakurai F, Inoue R, Nishino Y, Okuda A, Matsumoto O, Taga T, et al. Effect of DNA/liposome mixing ratio on the physicochemical characteristics, cellular uptake and intracellular trafficking of plasmid DNA/cationic liposome complexes and subsequent gene expression. J Control Release 2000;66:255–69.
[36] Song LY, Ahkong QF, Rong Q, Wang Z, Ansell S, Hope MJ, et al. Characterization of the inhibitory effect of PEG-lipid conjugates on the intracellular delivery of plasmid and antisense DNA mediated by cationic lipid liposomes. Biochim Biophys Acta 2002;1558:1–13.
[37] Deshpande MC, Davies MC, Garnett MC, Williams PM, Armitage D, Bailey L, et al. The effect of poly(ethylene glycol) molecular architecture on cellular interaction and uptake of DNA complexes. J Control Release 2004;97:143–56.
[38] Tachibana K, Uchida T, Ogawa K, Yamashita N, Tamura K. Induction of cell-membrane porosity by ultrasound. Lancet 1999;353:1409.
[39] Ishida O, Maruyama K, Sasaki K, Iwatsuru M. Size-dependent extravasation and interstitial localization of polyethyleneglycol liposomes in solid tumor-bearing mice. Int J Pharm 1999;190:49–56.
[40] Latz E, Schoenemeyer A, Visintin A, Fitzgerald KA, Monks BG, Knetter CF, et al. TLR9 signals after translocating from the ER to CpG DNA in the lysosome. Nat Immunol 2004;5:190–8.
[41] Leifer CA, Brooks JC, Hoelzer K, Lopez J, Kennedy MN, Mazzoni A, et al. Cytoplasmic targeting motifs control localization of toll-like receptor 9. J Biol Chem 2006;281:35585–92.
[42] Tousignant JD, Gates AL, Ingram LA, Johnson CL, Nietupski JB, Cheng SH, et al. Comprehensive analysis of the acute toxicities induced by systemic administration of cationic lipid: plasmid DNA complexes in mice. Hum Gene Ther 2000;11:2493–513.
[43] Meyer O, Schughart K, Pavirani A, Kolbe HV. Multiple systemic expression of human interferon-beta in mice can be achieved upon repeated administration of optimized pcTG90-lipoplex. Gene Ther 2000;7:1606–11.
[44] Donnelly JJ, Wahren B, Liu MA. DNA vaccines: progress and challenges. J Immunol 2005;175:633–9.
[45] Rice J, Ottensmeier CH, Stevenson FK. DNA vaccines: precision tools for activating effective immunity against cancer. Nat Rev Cancer 2008;8:108–20.
[46] Cook-Mills JM, Deem TL. Active participation of endothelial cells in inflammation. J Leukoc Biol 2005;77:487–95.
[47] Kolios G, Valatas V, Kouroumalis E. Role of Kupffer cells in the pathogenesis of liver disease. World J Gastroenterol 2006;12:7413–20.
[48] Higuchi Y, Kawakami S, Yamashita F, Hashida M. The potential role of fucosylated cationic liposome/NFkappaB decoy complexes in the treatment of cytokine-related liver disease. Biomaterials 2007;28:532–9.
[49] Wong J, Kubes P, Zhang Y, Li Y, Urbanski SJ, Bennett CF, et al. Role of ICAM-1 in chronic hepatic allograft rejection in the rat. Am J Physiol Gastrointest Liver Physiol 2002;283:196–203.

Chapter 33

Effective In Vitro and In Vivo Gene Delivery by the Combination of Liposomal Bubbles (Bubble Liposomes) and Ultrasound Exposure

Ryo Suzuki and Kazuo Maruyama

Abstract

Gene delivery with a physical mechanism using ultrasound (US) and nano/microbubbles is expected as an ideal system in terms of delivering plasmid DNA noninvasively into a specific target site. We developed novel liposomal bubbles (Bubble liposomes (BLs)) containing the lipid nanobubbles of perfluoropropane which were utilized for contrast enhancement in ultrasonography. BLs were smaller in diameter than conventional microbubbles and induced cavitation upon exposure ultrasound. In addition, when coupled with US exposure, BLs could deliver plasmid DNA into various types of cells in vitro and in vivo. The transfection efficiency with BLs and US was higher than that with conventional lipofection method. Therefore, the combination of BLs and US might be an efficient and novel nonviral gene delivery system.

Key words: Liposomes, Nanobubbles, Gene delivery, Ultrasound, Noninvasive, Nonviral vector

1. Introduction

Ultrasound (US) has been utilized as a useful tool for in vivo imaging, destruction of renal calculus and treatment for fibroid of the uterus. It was reported that US was proved to increase permeability of the plasma membrane and reduce the thickness of the unstirred layer of the cell surface, which encourages the DNA entry into cells (1, 2). The first studies applying ultrasound for gene delivery used frequencies in the range of 20–50 kHz (1, 3). However, these frequencies, along with cavitation, are also known to induce tissue damage if not properly controlled (4–6). To improve this problem, many studies using therapeutic ultrasound for gene delivery, which operates at frequencies of

Volkmar Weissig (ed.), *Liposomes*, Methods in Molecular Biology, vol. 605,
DOI 10.1007/978-1-60327-360-2_33, © Humana Press, a part of Springer Science+Business Media, LLC 2010

1–3 MHz, intensities of 0.5–2.5 W/cm², and pulse-mode have emerged (7–9). In addition, it was reported that the combination of therapeutic US and microbubble echo contrast agents could enhance gene transfection efficiency (10–14). In the sonoporation with microbubbles, it was reported that estimates of pore size based on the physical diameter of maker compounds were most commonly in the range of 30–100 nm, and estimates of membrane recovery time ranged from a few seconds to a few minutes (15). Therefore, it is thought that plasmid DNA is effectively and directly transferred into the cytosol via these pores. Conventional microbubbles including US contrast agents based on protein microspheres and sugar microbubbles are commercially available, the size of these bubbles being about 1–6 μm (16). For example, although the mean diameter of Optison microbubbles is about 2.0–4.5 μm, and they contain bubbles of up to 32 μm in diameter. Tsunoda et al. reported that some mice died immediately after the i.v. injection of Optison without ultrasound exposure due to lethal embolisms in vital organs (17). The same problem has not been reported in humans, but there is the possibility that Optison can not pass through capillary vessels. Therefore, microbubbles should generally be smaller than red blood cells. From this stand point of view, it is necessary to develop novel bubbles which are smaller than conventional microbubbles. Using liposome technology, we developed novel liposomal bubbles containing perfluoropropane gas. We called these bubbles "Bubble liposomes (BLs)." BLs were smaller than Optison (18–21). In addition, BLs could effectively deliver plasmid DNA by the combination with US exposure in vitro and in vivo.

2. Materials

2.1. Preparation of BLs (18)

1. 1,2-distearoyl-sn-glycero-phosphatidylcholone (DSPC) and 1,2-distearoyl-sn-glycero-3-phosphatidyl-ethanolamine-methoxypolyethyleneglycol (DSPE-PEG(2 k)-OMe) (NOF corporation, Tokyo, Japan).
2. Chloroform.
3. Diisopropyl ether.
4. Phosphate buffered saline (pH 7.4) (PBS): 137 mM NaCl, 8.10 mM Na_2HPO_4, 2.68 mM KCl, 1.47 mM KH_2PO_4 (Wako Pure Chemical Industries).
5. Perfluoropropane (Takachiho Chemical Industries, Tokyo, Japan).
6. Rotary evaporator (TOKYO RIKAKIKAI, Co. Ltd. (EYELA), Tokyo, Japan).

7. Extruding apparatus (Northern Lipids Inc., Vancouver, BC).
8. Bath-type sonicator (42 kHz, 100 W) (Branson Ultrasonics Co., Danbury, CT).
9. Liposome sizing filters (pore sizes: 100 and 200 nm) (Nuclepore Track-Etch Membrane, Whatman plc, UK).
10. 0.45 μm pore size filter (MILLEX HV filter unit, Durapore PVDF membrane) (Millipore Corporation, MA).
11. Dynamic light scattering (ELS-800) (Otsuka Electronics Co., Ltd., Osaka, Japan).
12. Phospholipid C-test wako (Wako Pure Chemical Industries).

2.2. Transmission Electron Microscopy of BLs (20)

1. Sodium alginate (500-600cP).
2. Calcium chloride.
3. Glutaraldehyde.
4. Cacodylate buffer.
5. Osmiumtetroxide.
6. Ethanol.
7. Epan812.
8. Uranyl acetate.
9. Electron microscope: JEOL JEM12000EX at 100 kV.

2.3. In Vitro Ultrasonography with BLs (19)

1. Ultrasound imaging equipment: UF-750XT (Fukuda Denshi Co. Ltd., Tokyo, Japan).
2. 9 MHz linear probe (9 MHz, Fukuda Denshi Co. Ltd.)

2.4. Gene Delivery with BLs and US In Vitro and In Vivo

1. Cells: COS-7 cells (the African green monkey kidney fibroblast cell line), S-180 cells (mouse sarcoma), Meth-A fibrosarcoma cells (mouse fibrosarcoma), Jurkat cells (human T cell line), Colon 26 cells (mouse colon adenocarcinoma), B16BL6 cells (mouse meranoma), Human umbilical vein endothelial cells (HUVEC) (Kurabo Industries, Osaka, Japan).
2. Culture media: Dulbecco's modified Eagle's medium (DMEM), RPMI-1640, Eagle's medium (MEM) and medium 199 (Sigma Chemical Co., St. Louis, MO), Supplements: Fetal bovine serum (FBS, GIBCO, Invitrogen Co., Carlsbad, CA), HEPES and heparin (Wako Pure Chemical Industries), endothelial cell growth supplement (ECGS) (Sigma Chemical Co.), Antibiotics: Penicillin and Streptomycin (Wako Pure Chemical Industries).
3. COS-7 cells and S-180 cells were cultured in DMEM supplemented with 10% heat-inactivated FBS. Meth-A fibrosarcoma cells and Jurkat cells were cultured with RPMI-1640 supplemented with 10% heat inactivated FBS. Colon 26 cells

were cultured with RPMI-1640 supplemented with 10% heat-inactivated FBS and 2.5% HEPES. B16BL6 cells were cultured with MEM supplemented with 10% heat-inactivated FBS. HUVECs were cultured in a DMEM and medium 199 mixture with 15% heat-inactivated FBS, heparin (3.25 U/mL) and ECGS. All culture media contained 100 U/ml penicillin and 100 μg/ml streptomycin.

4. Animals: ddY mice (4–6 weeks age, male), Anesthetic agent: NEMBUTAL (Dainippon Sumitomo Pharma Co., Ltd., Osaka, Japan), Adhesive agent (Aron Alpha) (Daiichi Sankyo Co., Ltd., Tokyo, Japan).
5. Ultrasound equipments and probes for gene delivery – Ultrasound equipments: Sonopore 3000 and Sonopore 4000 (NEPAGENE Co. Ltd.), Probe: KP-T6 (diameter: 6 mm) and KP-T8 (diameter: 8 mm), KP-T20 (diameter: 20 mm) (NEPAGENE Co., Ltd.)
6. Assessment of cytotoxicity: MTT [3-(4,5-s-dimethylthiazol-2-yl)-2,5-diphenyl tetrazolium bromide] (Dojindo, Kumamoto, Japan), Sodium dodecyl sulfate (SDS) (Wako Pure Chemical Industries), Microplate reader (POWERSCAN HT; Dainippon Pharmaceutical, Osaka, Japan).
7. Luciferase assay: Cell lysis buffer (0.1 M Tris–HCl (pH 7.8), 0.1% Triton X-100, 2 mM EDTA), Luciferase assay system (Promega, Madison, WI), Luminometer (TD-20/20) (Turner Designs, Sunnyvale, CA).
8. In vivo luciferase imaging: Escain (Mylan Inc., Tokyo, Japan), D-luciferin and In vivo luciferase imaging system (IVIS) (Caliper Life Sciences, MA).

3. Methods

3.1. Preparation of BLs (18)

1. DSPC and DSPE-PEG(2 k)-OMe were dissolved in 8 mL of 1:1 (v/v) chloroform/diisopropyl ether.
2. Four milliliter of PBS (pH 7.4) was added into the lipid solution. The mixture was sonicated to make suspension, and evaporated at 65° (water bath) to remove solvent.
3. After evaporation, liposome suspension was passed through sizing filters (pore sizes: 100 and 200 nm) using an extruding apparatus. And the size of liposomes was adjusted to less than 200 nm.
4. The liposomes suspension was sterilized by passing them through a 0.45 μm pore size filter. (see Fig. 1a)
5. Finally, size of the sterilized liposomes was measured with dynamic light scattering (ELS-800). The average diameter of

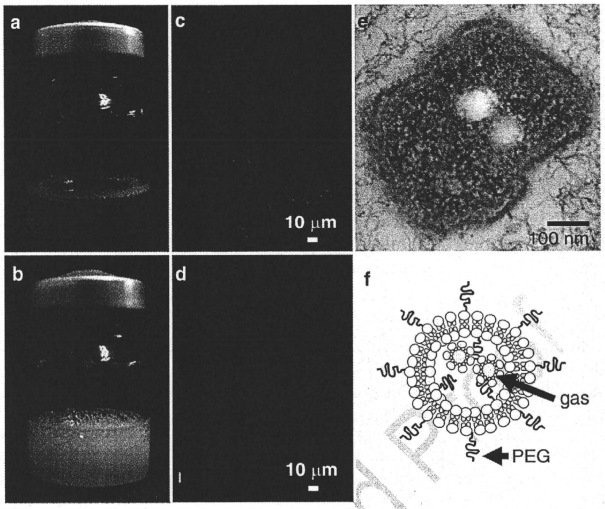

Fig. 1. Aspect and structure of BLs. PEG-liposomes (**a**) were sonicated with supercharged perfluoropropane gas. After that, they became to BLs (**b**). Optison (**c**) and BLs (**d**) were observed with microscope using the darklite illuminator (NEPAGENE, Co., Ltd). (**e**): Transmission electron microscopy (TEM) of BLs. (**f**): Scheme of structure of BLs

these liposomes were about 150–200 nm. In addition, lipid concentration was measured with the Phospholipid C-test wako.

6. The lipid concentration of liposomes suspension was adjusted to 1 mg/mL with PBS.
7. Two milliliter of the liposomes suspension (lipid conc. 1 mg/mL) was entered into sterilized vial (vial size: 5 mL).
8. The vial was filled with perfluoropropane, capped and then supercharged with 7.5 mL of perfluoropropane.
9. The vial was placed in a bath-type sonicator (42 kHz, 100 W) for 5 min to form BLs (see Fig. 1 and Note 1).

3.2. Transmission Electron Microscopy of BLs (20)

1. BLs were suspended into sodium alginate (500-600cP) solution (0.2% (w/v) in PBS).
2. This suspension was dropped into calcium chloride solution (100 mM in PBS) to hold BLs within calcium alginate gel.
3. The beads of calcium alginate gel containing BLs were prefixed with 2% glutaraldehyde solution in 0.1 M Cacodylate buffer.
4. The beads were postfixed with 2% OsO_4, dehydrated with an ethanol series, and then embedded in Epan812 (polymerized at 60°).

BookID 152219_ChapID 33_Proof# 1 - 03 / 10 / 2009

5. Ultrathin sections were made with an ultramicrotome at a thickness of 60–80 nm.
6. Ultrathin sections were mounted on 200 mesh copper grids.
7. They were stained with 2% uranyl acetate for 5 min and Pb for 5 min.
8. The samples were observed with JEOL JEM12000EX at 100 kV (see Fig. 1e; Notes 2 and 3).

3.3. In Vitro Ultrasonography with BLs (19)

1. BLs were placed into latex tube filled with degassed PBS (10 mL) in a water bath.
2. The probe (9 MHz) of an ultrasound imaging equipment was positioned under the water bath.
3. BLs in the tube were imaged (see Fig. 2 a, b).

3.4. In Vitro Gene Delivery with BLs and US

3.4.1. Transfection of Plasmid DNA into Cells with BLs and US (21)

1. Plasmid DNA, cells and BLs were suspended in culture medium with 10% FBS (final volume; 500 μL) in 2 mL polypropylene tubes.
2. The probe (KP-T6) (2 MHz, diameter: 6 mm) of US was placed into the suspension.
3. US was exposed to the suspensions with Sonopore 3000 or 4000 under the condition of various US parameters (Duty, Intensity, Exposure time, Burst rate) (see Fig. 2c).

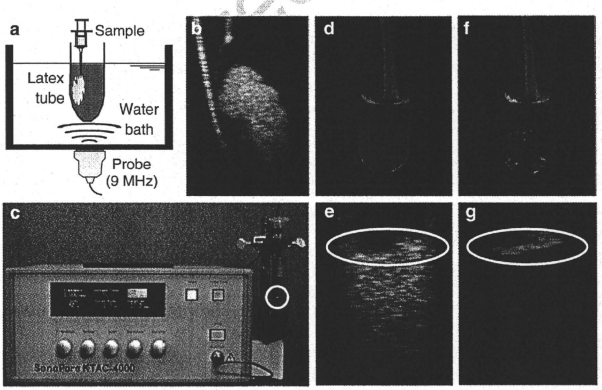

Fig. 2. In vitro Ultrasonography with BLs. The Method of ultrasonography for observation of BLs was shown in (**a**). BLs were injected into PBS filled latex tube in the water bath. Then, the samples were observed with ultrasonography (**b**). To confirm the disruption of BLs by US exposure using Sonopore 4000 (**c**), BLs were observed with naked image (**d**, **f**) and ultrasonography (**e**, **g**) before (**d**, **e**) and after (**f**, **g**) US exposure (2 MHz, 2.5 W/cm^2, 10 s). *Circle* in (**c**, **e**, **g**) shows US probe

4. After US exposure, the cells were washed twice with PBS and then resuspended in fresh culture medium.
5. The cells were cultured in culture plate or wells.
6. After 2 days culture of cells, the expression of transgene was measured (see Fig. 3; Notes 4 and 5).

3.4.2. Assessment of Cytotoxicity by the Treatment of BLs and US to Cells (18)

1. Cells (1×10^5) and BLs were suspended in culture medium with 10% FBS (final volume; 500 μL) in 2 mL polypropylene tubes.
2. US was exposed to cells using Sonopore 3000 or 4000 with a probe (KP-T6) (2 MHz, diameter: 6 mm).
3. After US exposure, the cells were washed twice with PBS and then resuspended in fresh culture medium.
4. One hundred microliter of the cells suspension were cultured in 96 well plates for 24 h.
5. Cell viability was assayed using MTT, as described by Mosmann, with minor modifications (22). Briefly, MTT (5 mg/mL, 10 μL) was added to each well, and the cells were incubated at 37°C for 4 h. The formazan product was dissolved in 100 μL of 10% SDS containing 15 mM HCl. Color intensity was measured using a microplate reader at test and reference wavelengths of 595 and 655 nm, respectively.

3.5. In Vivo Gene Delivery with BLs and US

3.5.1. Gene Delivery for Femoral Artery (18)

1. The femoral artery was exposed by operation.
2. BLs (250 μg) and plasmid DNA (10 μg) suspension (300 μL) was slowly injected into the femoral artery of ddY mice (6 weeks age, male) using 30-gauge needle (M-S Surgical MFG. Co. Ltd., Tokyo, Japan).
3. In the same time, US (frequency: 1 MHz, duty: 50%, intensity: 1 W/cm^2, time: 2 min) was transdermally exposed to downstream of injection site using Sonopore 3000 or 4000 with a probe (KP-T8) (diameter: 8 mm). [AU1]
4. After 2 days of injection, the mice were sacrificed and the femoral artery of US exposure area was collected. Then, gene expression in the artery was measured (see Fig. 4; Notes 6 and 7).

3.5.2. Gene Delivery for Ascites Tumor (20)

1. S-180 cells (1×10^6 cells) were i.p. injected into ddY mice (4 weeks age, male) on day 0.
2. When S-180 cells grew as the ascites tumor in mice after 8 days of the injection, the mice were anaesthetized with NEMBUTAL Injection (50 mg/kg), then injected with 510 μL of plasmid DNA and BLs (500 μg) in PBS.
3. US (frequency: 1 MHz, duty: 50%, intensity: 1 W/cm^2, time: 1 min) was transdermally exposed to the abdominal area using Sonopore 300 or 4000 with a probe (KP-S20) (diameter: 20 mm).

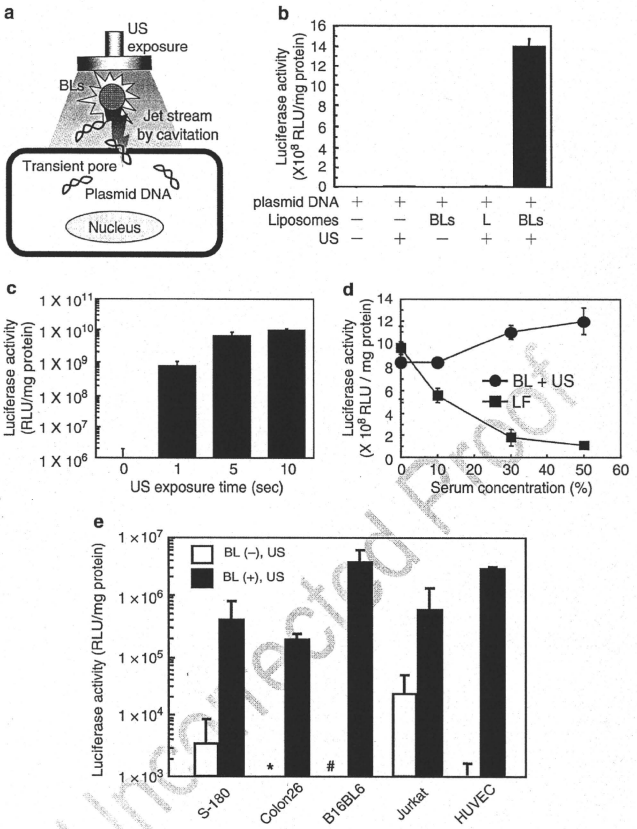

Fig. 3. Property of gene delivery with BLs and US exposure (**a**) Schema of transfection mechanism by BLs and US. The mechanical effect based on the disruption of BLs by US exposure, which results in generation of some pores on plasma membrane, is associated with direct delivery of extracellular plasmid DNA into cytosol. (**b**) Luciferase expression in COS-7 cells transfected by BLs and US. COS-7 cells (1×10^5 cells/500 μL/tube) were mixed with pCMV-Luc (5 μg) and BLs (60 μg). The cell mixture was exposed with US (Frequency: 2 MHz, Duty: 50%, Burst rate: 2 Hz, Intensity: 2.5 W/cm^2, Time: 10 s). The cells were washed and cultured for 2 days. After that, luciferase activity was measured. (**c**) Effect of US condition on transfection efficiency with BLs. COS-7 cells were exposed with US (Frequency: 2 MHz, Duty: 50%, Burst rate: 2 Hz, Intensity: 2.5 W/cm^2, Time: 0, 1, 5, 10 s) in the presence of pCMV-Luc (0.25 μg) and BLs (60 μg). Luciferase activity was measured as above. (**d**) Effect of serum on transfection efficiency of BLs. COS-7 cells in the medium containing FBS (0, 10, 30, 50% (v/v)) were treated with US (Frequency: 2 MHz, Duty: 50%, Burst rate: 2 Hz, Intensity: 2.5 W/cm^2, Time: 10 s), pCMV-Luc (0.25 μg) and BLs (60 μg) or transfected with lipoplex of pCMV-Luc (0.25 μg) and lipofectin (1.25 μg). (**e**) In vitro gene delivery to various types of cell using BLs and US. The method of gene delivery was same as above. S-180: mouse sarcoma cells, Colon26: mouse colon adenocarcinoma cells, B16BL6: mouse melanoma cells, Jurkat: human T cell line, HUVEC: human umbilical endothelial cells. Luciferase activity was measured as above. * $<10^3$RLU/mg protein, # $<10^6$RLU/mg protein Each data represents the mean ± S.D. ($n=3$). L: PEG-liposomes, LF: Lipofectin

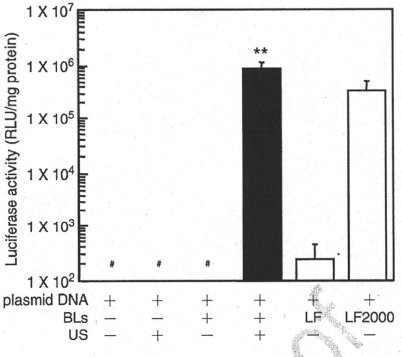

Fig. 4. In vivo gene delivery into mouse ascites tumor cells with Bubble liposomes. S-180 cells (1×10^6 cells) were i.p. injected into ddY mice. After 8 days, the mice were anaesthetized, then injected with 510 μL of pCMV-Luc (10 μg) and Bubble liposomes (500 μg) in PBS. Ultrasound (frequency: 1 MHz, duty: 50%; intensity: 1.0 W/cm^2, time: 1 min) was transdermally applied to the abdominal area. In another experiment, pCMV-Luc (10 μg) – Lipofectin (50 μg) or Lipofectamine 2000 (50 μg) complex was suspended in PBS (510 μL) and injected into the peritoneal cavity of mice. After 2 days, S-180 cells were recovered from the abdomens of the mice. Luciferase activity was determined, as described in Materials and Methods. Each bar represents the mean ± S.D. (n=3–6). **P<0.01 compared to the group treated with plasmid DNA, Bubble liposomes, ultrasound exposure or lipofection with Lipofectin or Lipofectamine 2000. LF, Lipofectin. LF2000, Lipofectamine 2000. # < 10^2 RLU/mg protein

4. After 2 days of US exposure, ascites tumor cells were recovered from the abdomen of the mice. Then, the gene expression in the recovered cells was measured (see Fig. 5).

3.5.3. Gene Delivery for Solid Tumor (20)

1. S-180 cells (1×10^6 cells) were inoculated into the left footpad of ddY mice (5 weeks age, male).
2. At day 4, when the thickness of the footpad was over 3.5 mm (normal thickness was about 2 mm), the left femoral artery was exposed by operation.
3. BLs (100 μg) and plasmid DNA suspension (100 μL) were injected into the femoral artery using 30-gauge needle.
4. In the same time, US (frequency: 0.7 MHz, duty: 50%, intensity: 1.2 W/cm^2, time: 2 min) was transdermally exposed to the tumor tissue using Sonopore 3000 or 4000 with a probe (KP-T8) (diameter: 8 mm).
5. The needle hole was then closed with an adhesive agent and skin was put in a suture.

BookID 152219_ChapID 33_Proof# 1 - 03 / 10 / 2009

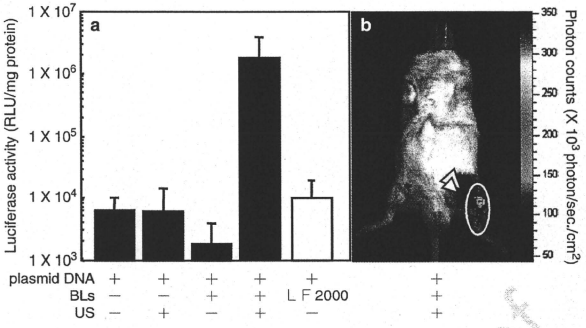

Fig. 5. Gene delivery to femoral artery with Bubble liposomes Each sample containing plasmid DNA 10 μg was injected into femoral artery. At the same time, ultrasound (frequency, 1 MHz; duty, 50%; burst rate, 2 Hz; intensity, 1 W/cm^2; time 2 min) was exposed to the downstream area of injection site. (**a**) Luciferase expression in femoral artery of the ultrasound exposure area at 2 days after transfection, Luciferase expression was determined as described in Materials and Methods. Data are shown as means ± S.D. (n=5). (LF2000: Lipofectamine 2000) (**b**) In vivo luciferase imaging at 2 days after transfection in the mouse treated with plasmid DNA, Bubble liposomes and ultrasound exposure. The photon counts are indicated by the pseudocolor scales

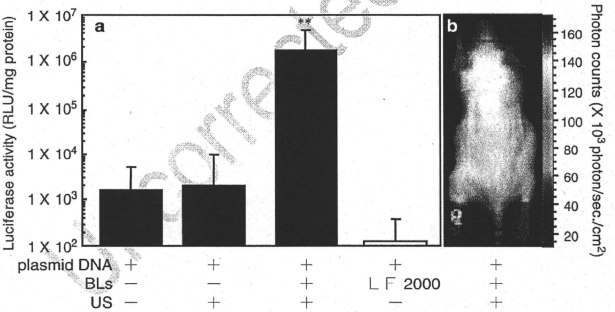

Fig. 6. In vivo gene delivery into mouse solid tumor with Bubble liposomes. S-180 cells (1 × 10^6 cells) were inoculated into left footpad of ddY mice. After 4 days, the mice were anaesthetized, then injected with 100 μL of pCMV-Luc (10 μg) in absence or presence of Bubble liposomes (100 μg) in PBS. Ultrasound (frequency: 0.7 MHz, duty: 50%; intensity: 1.2 W/cm^2, time: 1 min) was transdermally exposed to tumor tissue. In another experiment, pCMV-Luc (10 μg) – Lipofectamine 2000 (25 μg) complex was suspended in PBS (100 μL) and injected into the left femoral artery. After 2 days, tumor tissue was recovered from the mice. Luciferase activity was determined as described in Materials and Methods. (**a**) Luciferase activity in solid tumor. Each bar represents the mean ± S.D. for five mice/group. **P<0.01 compared to the group treated with plasmid DNA, ultrasound exposure or Lipofectamine 2000. (**b**) In vivo luciferase imaging in the solid tumor bearing mice. The photon counts are indicated by the pseudocolor scales. LF 2000, Lipofectamine 2000

6. After 2 days of US exposure, the mice were sacrificed and the tumor tissues were collected. Then, the gene expression of the tumor tissue was measured (see Fig. 6 and Note 8).

3.6. Measurement of Reporter Gene Expression

3.6.1. Luciferase Assay

1. The lysis buffer (0.1 M Tris–HCl (pH 7.8), 0.1% Triton X-100, 2 mM EDTA) was added to the sample cells in vitro or tissues in vivo. In the case of the tissues in vivo, they were homogenized before next step.
2. The cells or the homogenized tissues in lysis buffer were repeatedly frozen and thawed three times to completely disrupt the cell membranes.
3. After that, the lysate of the cells or tissues was centrifuged and the supernatant was collected in other tube.
4. Luciferase activity in the supernatant was measured using a luciferase assay system and a luminometer. The activity is reported in relative light units (RLU) per mg protein of cells or tissue.

3.6.2. In Vivo Luciferase Imaging

1. The mice were anaesthetized with Escain and i.p. injected with D-luciferin (150 mg/kg).
2. After 10 min, luciferase expression was observed with in vivo luciferase imaging system (IVIS).

4. Notes

1. There are some important points to prepare BLs. The air in the vial containing the liposome suspension is completely replaced with perfluoropropane. After that, it needs to be supercharged in the vial with perfluoropropane. And the vial is sonicated with a bath-type sonicator (42 KHz, 100 W) (BRANSONIC 2510 J-DTH, Branson Ultrasonics). In this step, sonication power and the vial position in the bath are very important. Because we have experimented that BLs were not prepared using other type of bath sonicator (UC-1 (38 KHz, 80 W), IKEDA RIKA, Japan) with low intensity of ultrasound exposure. In addition, BLs were not prepared using other gas such as air, nitrogen gas or carbonic dioxide gas. Therefore, it thought that it is important for the preparation of BL to use hydrophobic gas such as perfluoropropane.
2. To fix BLs as a sample for transmission electron microscope, BLs were held within calcium alginate gel. The handling of BLs was improved by holding within the gel. The advantage for using this gel is to make the gel even at low temperature. Because BLs became unstable according to increasing temperature. Therefore, it is thought that the gel, such as agarose, which has gel point at high temperature is inappropriate for this purpose.
3. It was thought that liposomes were reconstituted by sonication under the condition of supercharge with perfluoropropane.

Then, perfluoropropane was entrapped within lipids like micelles. In addition, the lipid nanobubbles were encapsulated within liposomes. To confirm the structure of BLs, we observed BLs with transmission electron microscope. Interestingly, BLs had nanobubbles into lipid bilayer. Therefore, we called this "Bubble liposome" because of this structure. This structure of BLs was different from that of conventional microbubbles and nanobubbles which had lipid monolayer.

4. This protocol can be adapted for many other types of cell. In the gene transfection for adherent cells, the transfection efficiency in the condition of suspension was higher than that in the condition of adhesion on the culture plate. Although this result is unclear, it is thought that the distance between BLs and cells is important. Because BLs entrapping gas is easy to flow and result in getting away from the adherent cells on the plate.
5. In in vitro gene delivery, it is very important to fix the location of it, in order to reduce the experimental error of each data. The efficiency of this gene delivery was not affected even in the presence of serum. Moreover, the gene expression was observed even under the condition of US exposure for 1 s. From these results, it was suggested that this system could immediately deliver plasmid DNA into cells.
6. In in vivo gene delivery, echo jelly is necessary for US exposure to mice. Gene expression was observed in the arrested area of US exposure. Because it is thought that the mechanical effect based on the disruption of BLs by US exposure results in generation of some pores on plasma membrane of the cells in the area of US exposure.
7. This system is thought that there is not a serious damage for the cells in blood such as red blood cells by the disruption of BLs in blood stream by US exposure.
8. The transfection efficiency with the gene delivery system by sonoporation mechanism using BLs and US was higher than conventional lipofection method with Lipofectin and Lipofectamine 2000. Therefore, it is expected that this system might be an effective nonviral gene delivery system.

Acknowledgements

We are grateful to Dr. Katsuro Tachibana (Department of Anatomy, School of Medicine, Fukuoka University) for technical advice regarding the induction of cavitation with ultrasound, to Dr. Naoki Utoguchi, Mr. Yusuke Oda, Mr. Eisuke Namai,

Ms. Tomoko Takizawa, Ms. Kaori Sawamura and Ms. Kumiko Tanaka (Department of Pharmaceutics, School of Pharmaceutical Sciences, Teikyo University), Yoichi, Negishi (School of Pharmacy, Tokyo University of Pharmacy and Life Science), and Dr. Kosuke Hagisawa (Department of Medical Engineering, National Defense Medical College) for excellent technical advice and assistance, to Mr. Yasuhiko Hayakawa, Mr. Takahiro Yamauchi, and Mr. Kosho Suzuki (NEPAGENE Co., Ltd.) for technical advice regarding ultrasound exposure using Sonopore 3000 and 4000, and Sonitron 2000.

This study was supported by an Industrial Technology Research Grant in 2004 from NEDO, JSPS KAKENHI (16650126), MEXT KAKENHI (160700392, 19700423), a Research on Advanced Medical Technology (17070301) in Health and Labour Sciences Research Grants from Ministry of Health, Labour and Welfare, and the Program for Promotion of Fundamental Studies(07-24) in Health Sciences of the National Institute of Biomedical Innovation (NIBIO).

References

1. Fechheimer M, Boylan JF, Parker S, Sisken JE, Patel GL, Zimmer SG (1987) Transfection of mammalian cells with plasmid DNA by scrape loading and sonication loading. Proc Natl Acad Sci U S A 84:8463–8467
2. Miller MW, Miller DL, Brayman AA (1996) A review of in vitro bioeffects of inertial ultrasonic cavitation from a mechanistic perspective. Ultrasound Med Biol 22:1131–1154
3. Joersbo M, Brunstedt J (1990) Protein synthesis stimulated in sonicated sugar beet cells and protoplasts. Ultrasound Med Biol 16:719–724
4. Miller DL, Pislaru SV, Greenleaf JE (2002) Sonoporation: mechanical DNA delivery by ultrasonic cavitation. Somat Cell Mol Genet 27:115–134
5. Guzman HR, McNamara AJ, Nguyen DX, Prausnitz MR (2003) Bioeffects caused by changes in acoustic cavitation bubble density and cell concentration: a unified explanation based on cell-to-bubble ratio and blast radius. Ultrasound Med Biol 29:1211–1222
6. Wei W, Zheng-zhong B, Yong-jie W, Qing-wu Z, Ya-lin M (2004) Bioeffects of low-frequency ultrasonic gene delivery and safety on cell membrane permeability control. J Ultrasound Med 23:1569–1582
7. Duvshani-Eshet M, Machluf M (2005) Therapeutic ultrasound optimization for gene delivery: a key factor achieving nuclear DNA localization. J Control Release 108:513–528
8. Tata DB, Dunn F, Tindall DJ (1997) Selective clinical ultrasound signals mediate differential gene transfer and expression in two human prostate cancer cell lines: LnCap and PC-3. Biochem Biophys Res Commun 234:64–67
9. Kim HJ, Greenleaf JF, Kinnick RR, Bronk JT, Bolander ME (1996) Ultrasound-mediated transfection of mammalian cells. Hum Gene Ther 7:1339–1346
10. Greenleaf WJ, Bolander ME, Sarkar G, Goldring MB, Greenleaf JF (1998) Artificial cavitation nuclei significantly enhance acoustically induced cell transfection. Ultrasound Med Biol 24:587–595
11. Shohet RV, Chen S, Zhou YT, Wang Z, Meidell RS, Unger RH, Grayburn PA (2000) Echocardiographic destruction of albumin microbubbles directs gene delivery to the myocardium. Circulation 101:2554–2556
12. Taniyama Y, Tachibana K, Hiraoka K, Namba T, Yamasaki K, Hashiya N, Aoki M, Ogihara T, Yasufumi K, Morishita R (2002) Local delivery of plasmid DNA into rat carotid artery using ultrasound. Circulation 105:1233–1239
13. Taniyama Y, Tachibana K, Hiraoka K, Aoki M, Yamamoto S, Matsumoto K, Nakamura T, Ogihara T, Kaneda Y, Morishita R (2002) Development of safe and efficient novel nonviral gene transfer using ultrasound: enhancement of transfection efficiency of naked plasmid DNA in skeletal muscle. Gene Ther 9:372–380

14. Sonoda S, Tachibana K, Uchino E, Okubo A, Yamamoto M, Sakoda K, Hisatomi T, Sonoda KH, Negishi Y, Izumi Y, Takao S, Sakamoto T (2006) Gene transfer to corneal epithelium and keratocytes mediated by ultrasound with microbubbles. Invest Ophthalmol Vis Sci 47:558–564
15. Newman CM, Bettinger T (2007) Gene therapy progress and prospects: ultrasound for gene transfer. Gene Ther 14:465–475
16. Lindner JR (2004) Microbubbles in medical imaging: current applications and future directions. Nat Rev Drug Discov 3:527–532
17. Tsunoda S, Mazda O, Oda Y, Iida Y, Akabame S, Kishida, T, Shin-Ya M, Asada H, Gojo S, Imanishi J, Matsubara H, Yoshikawa T (2005) Sonoporation using microbubble BR14 promotes pDNA/siRNA transduction to murine heart. Biochem Biophys Res Commun 336:118–127
18. Suzuki R, Takizawa T, Negishi Y, Hagisawa K, Tanaka K, Sawamura K, Utoguchi N, Nishioka T, Maruyama K (2007) Gene delivery by combination of novel liposomal bubbles with perfluoropropane and ultrasound. J Control Release 117:130–136
19. Suzuki R, Takizawa T, Negishi Y, Utoguchi N, Maruyama K (2007) Effective gene delivery with liposomal bubbles and ultrasound as novel non-viral system. J Drug Target 15:531–537
20. Suzuki R, Takizawa T, Negishi Y, Utoguchi N, Sawamura K, Tanaka K, Namai E, Oda Y, Matsumura Y, Maruyama K (2008) Tumor specific ultrasound enhanced gene transfer in vivo with novel liposomal bubbles. J Control Release 125:137–144
21. Suzuki R, Takizawa T, Negishi Y, Utoguchi N, Maruyama K (2008) Effective gene delivery with novel liposomal bubbles and ultrasonic destruction technology. Int J Pharm 354:49–55
22. Mosmann T (1983) Rapid colorimetric assay for cellular growth and survival: application to proliferation and cytotoxicity assays. J Immunol Methods 65:55–63

Ultrasonics Sonochemistry 18 (2011) 425–430

Contents lists available at ScienceDirect

Ultrasonics Sonochemistry

journal homepage: www.elsevier.com/locate/ultsonch

Synergistic effect of ultrasound and antibiotics against *Chlamydia trachomatis*-infected human epithelial cells in vitro

Yurika Ikeda-Dantsuji [a], Loreto B. Feril Jr. [a,*], Katsuro Tachibana [a], Koichi Ogawa [a], Hitomi Endo [a], Yoshimi Harada [a], Ryo Suzuki [b], Kazuo Maruyama [b]

[a] Department of Anatomy, Fukuoka University School of Medicine, Fukuoka, Japan
[b] Department of Biopharmaceutics, School of Pharmaceutical Sciences, Teikyo University, Kanagawa, Japan

ARTICLE INFO

Article history:
Received 12 April 2010
Received in revised form 12 July 2010
Accepted 21 July 2010
Available online 27 July 2010

Keywords:
Ultrasound
Nanobubbles
Antibiotic
Intracellular bacteria

ABSTRACT

To investigate whether or not the combined ultrasound and antibiotic treatment is effective against chlamydial infection, a new ultrasound exposure system was designed to treat chlamydia-infected cells. First, the minimum inhibitory concentrations of antibiotics against *Chlamydia trachomatis* were determined. Infected cultures were treated with antibiotics then sonicated at intensity of 0.15 or 0.44 W/cm^2 with or without Bubble liposomes. After 48 or 72 h after infection, chlamydial inclusions were stained and examined by fluorescence microscopy. The internalization of dextran–fluorescein conjugates by ultrasound irradiation with Bubble liposomes was observed by fluorescence microscopy. The results showed that application of nanobubble-enhanced ultrasound caused no significant effect on cell viability and chlamydial infectivity. However, Doxycycline (1/2 MIC) or CZX (1.0 μg/ml) in combination with nanobubble-enhanced ultrasound dramatically reduced the number of inclusions compared with that administered with antibiotics only. Bubble dose-dependent synergy was also observed. After ultrasound irradiation at intensity of 0.44 W/cm^2 on the presence of Bubble liposomes, 10% of HeLa cells were observed to have internalized the dextran molecules. This study suggests the possibility of using nanobubble-enhanced ultrasound to deliver antibiotic molecules into cells to eradiate intracellular bacteria, such as chlamydiae, without causing much damage to the cells itself.

1. Introduction

An obligate intracellular pathogen, *Chlamydia trachomatis*, is the most prevalent sexually transmitted bacterium worldwide [1]. *C. trachomatis* is a Gram-negative bacterium which has a unique biphasic developmental cycle characterized by an infectious but metabolically inactive extracellular form, called the 'elementary body', which initiates infection through the uptake by the host cell. Thereafter, elementary bodies differentiate into noninfectious but metabolically active forms, called the 'reticulate body', which proliferate within the inclusion. Reticulate bodies also differentiate back to elementary bodies before release at the end of the developmental cycle. At its sites of primary infection, *C. trachomatis* infects the urethral or cervical epithelium, causing acute urethritis or cervicitis [2]. These frequently progress into chronic inflammatory disease, the most significant of which, is chronic salpingitis, an inflammatory disease of fallopian tubes that can result in pelvic inflammatory disease, ectopic pregnancy, and tubal infertility [3].

The recommended antibiotic treatments for urogenital infections are a single dose of azithromycin or a 7-day course of doxycycline for management of active infections [4]. These regimens have been shown to result in satisfactory cure rates of acute infections [5,6]; however, chronic diseases (designated "persistent infection") have been suggested to be less responsive to antibiotic therapy [7].

Previous work has shown that some antibiotics treatment of *Pseudomonas aeruginosa* or *Escherichia coli* coupled with ultrasound irradiation enhances the bactericidal activity [8]. The more recent research has revealed that similar synergistic effects of combined ultrasound and antibiotic treatment are seen in both Gram-positive and Gram-negative bacteria with some antibiotics, especially the aminoglycosides [9]. It is not clear whether the combined ultrasound and antibiotic treatment are effective on intracellular pathogen, e.g. chlamydial infection. If an intracellular bacterial infection could be efficiently eradicated from an infected person, one could avoid chronic antibiotic treatments. In addition, this strategy of treatment could be beneficial in the management of chlamydial persistent diseases.

Here, we are studying the synergistic use of ultrasound and antibiotics to kill the *chlamydia*. This report presents results of

* Corresponding author. Address: 7-45-1 Nanakuma, Jonan-ku, Fukuoka 814-0180 Japan. Tel.: +81 92 801 1011x3206; fax: +81 92 865 6032.
E-mail addresses: ferilism@yahoo.com, feril@fukuoka-u.ac.jp (L.B. Feril).

1350-4177/$ - see front matter © 2010 Elsevier B.V. All rights reserved.
doi:10.1016/j.ultsonch.2010.07.015

the first step in that research, which is investigation of the in vitro response of *C. trachomatis*-infected human epithelial cells to combination of ultrasound and two types of antibiotics.

2. Materials and methods

2.1. Chlamydial strain and cell lines

C. trachomatis serovar E/UW-5/Cx was prepared in McCoy cells and propagated according to a previously reported method [10]. The mouse fibroblast cell line McCoy cell (CRL 1696) and human epithelial cell line HeLa 229 cell (CLL 2.1) were maintained in Dulbecco's modified Eagle medium (DMEM, Invitrogen, Grand Island, NY, USA) supplemented with 10% heat-inactivated fetal calf serum (FCS, Invitrogen) and 100 μg/ml streptomycin.

2.2. Infection of HeLa cells

The HeLa cells were seeded into a 24-well plate with lumox™ fluorocarbon film base (optically clear, 50 μm-thin, gas permeable film, Greiner bio-one, Gottingen, Germany). Stocks of chlamydial strain were diluted with sucrose–phosphate–glutamate (SPG) medium [10]. Chlamydial suspensions of 0.5×10^4 inclusion-forming units (IFUs) in 0.25 ml SPG medium were inoculated onto the monolayer cultures of HeLa cells (1×10^4 cells/well). This is equivalent to a multiplicity of infection of 0.5. After incubation at 37 °C for 90 min, the inoculum was decanted, and the cells were washed in medium to remove the nonadsorbed chlamydiae and were then further incubated in 1 ml DMEM containing 1 μg/ml cycloheximide (Sigma Chemicals, St. Louis, MO, USA) and 2% FCS (maintenance medium).

2.3. Preparation of bubble liposome

Bubble liposomes were prepared according to a method previously described [11]. Liposomes composed of 1,2-distearoyl-sn-glycero-phosphatidylcholine (DSPC) (NOF Corp., Tokyo, Japan) and 1,2-distearoyl-snglycero-3-phosphatidyl-ethanolamine-methoxypolyethyleneglycol(DSPE-PEG(2k)-OMe, (PEG Mw = ca. 2000), NOF) (94: 6 (m/m)) were prepared by reverse phase evaporation. Briefly, all reagents (totallipid: 100 μmol) were dissolved in 8 ml of 1:1 (v/v) chloroform/diisopropyl ether, then 4 ml of phosphate buffered saline (PBS) were added. The mixture was sonicated and evaporated at 65 °C. The solvent was completely removed, and the size of the liposomes was adjusted to less than 200 nm using an extruding apparatus (Northern Lipids Inc., Vancouver, BC, Canada) and sizing filters (pore sizes: 100 and 200 nm; Nuclepore Track-Etch Membrane, Whatman plc, UK). After sizing, the liposomes were sterilized by passing them through a 0.45 μm pore size filter (MILLEX HV filter unit, Durapore PVDF membrane, Millipore Corp., MA, USA). The size of the liposomes was measured by dynamic light scattering (ELS-800, Otsuka Electronics Co., Ltd., Osaka, Japan). The average diameter of these liposomes was between 150 and 200 nm. Lipid concentration was measured using the Phospholipid C test (Wako Pure Chemical Industries). BLs were prepared from the liposomes and perfluoropropane gas (Takachiho Chemical Industrial Co., Ltd., Tokyo, Japan). Briefly, 5 ml sterilized vials containing 2 ml of the liposome suspension (lipid concentration: 2 mg/ml) were filled with perfluoropropane, capped, and then supercharged with 7.5 ml of perfluoropropane. The vial was placed in a bath-type sonicator (42 kHz, 100 W; BRANSONIC 2510J-DTH, Branson Ultrasonics Co., Danbury, CT, USA) for 5 min to form the BLs. In this method, the liposomes were reconstituted by sonication under the condition of supercharge with perfluoropropane in the 5 ml vial container. At the same time, perfluoropropane would be entrapped within lipids like micelles, which were made by DSPC and DSPE-PEG(2k)-OMe from liposome composition, to form nanobubbles. The lipid nanobubbles were encapsulated within the reconstituted liposomes, which sizes were changed into around 1 μm from 150 to 200 nm of original.

2.4. Immunofluorescence staining and fluorescence microscopy

At 48 or 72 h after infection, the infected monolayers were washed with PBS, and the cells were fixed with −20 °C chilled methanol. After the specimens had been dried, the inclusion bodies were stained with fluorescein isothiocyanate (FITC)-labeled monoclonal antibody against *C. trachomatis* lipopolysaccharides (Progen Biotechnik, Heidelberg, Germany) for 30 min at room temperature. The cells were rinsed with saline, and the films were cut off from the plate, and mounted in a 1:1 solution of PBS–glycerol. The antibody staining resulted in yellow–green chlamydial proteins, and Evans blue counterstaining yielded red eukaryotic cells. The formation of inclusions was assessed using a Zeiss Axiophot fluorescence microscope. The cells positive for inclusions are considered infected cells and infectivity was presented as the number of inclusion-forming units (IFUs).

2.5. Antibiotics and measurements of MICs

Doxycycline (DOX, Sigma Chemicals) and ceftizoxime (CZX, Fujisawa Yakuhin Kogyou, Tokyo, Japan) were obtained in powder form. Both antibiotics were diluted with saline, and were dissolved in maintenance medium at a concentration of 100 μg/ml and frozen at −80 °C until used. The minimum inhibitory concentrations (MICs) were determined using a method previously described [12]. Briefly, confluent monolayer cultures of cells in a 24-well flat-bottomed plate with 13-mm coverslips were inoculated by centrifugation and incubated in 1 ml of maintenance medium containing a serial dilution of antibiotics for 72 h. To determine the MICs, the cover slips were stained and observed as described in Immunofluorescence staining and fluorescence microscopy. The lowest concentration of the antimicrobial agent that completely inhibited the formation of visible chlamydial inclusions was determined as the MIC.

2.6. Ultrasound exposure

An acoustically transparent gel (Pharmaceutical Innovations Inc., Newark, NJ) was applied on the ultrasound probe before positioning the plate containing the sample on top of it (Fig. 1). Thera-

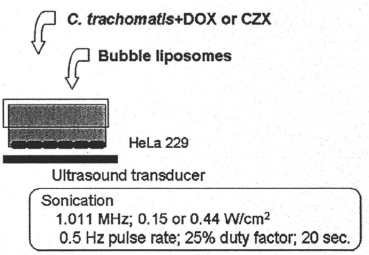

Fig. 1. Experimental design. Schematic drawing of the ultrasound setting. *C. trachomatis*-infected HeLa cells were exposed to ultrasound after addition of antibiotic and Bubble liposomes.

peutic ultrasound (1.011 MHz) was irradiated from a device (Sono-Pore KTAC-4000, NepaGene, Chiba, Japan) at intensity of 0.15 or 0.44 W/cm^2 (duty cycle of 25%) for 20 s immediately after addition of Bubble liposomes into the sample.

2.7. Measurement of cell viability

The Trypan blue dye exclusion test was carried out by mixing 200 μl of the suspension of HeLa cells with an equal amount of 0.3% Trypan blue solution (Sigma Chemicals) in PBS. After 5 min incubation at room temperature, the number of cells excluding Trypan blue was counted using a C-Chip disposable hemocytometer (Digital Bio Technology Co., Gyeonggi, Korea) to estimate the number of viable cells immediately after sonication.

2.8. Measurement of infectivity of chlamydiae

The 1.0 ml of chlamydial suspensions in SPG treated with ultrasound and/or nanobubbles was inoculated into triplicate cultures of McCoy cells in order to estimate the infectivity immediately after sonication. Chlamydial suspensions, 0.25 ml each, were added onto the monolayer culture of McCoy cells. After centrifugation at 1000*g* for 60 min, the inoculum was decanted, and the cells were washed with medium to remove the nonadsorbed chlamydiae, and were then further incubated in 1.0 ml of maintenance medium.

2.9. Internalization of dextran–fluorescein conjugates

Dextran–fluorescein conjugates (3000 MW, anionic: Molecular Probes, Inc., OR, USA) were soluble in 0.02 M Tris–HCl buffer (pH 8.0) at 10 μg/ml, and performed by filtration using 0.2 μm pore-diameter sterile filters. Aqueous solutions of dextran were diluted to 10 μg/ml with maintenance medium. The 50 μl of solution of dextran conjugates instead of antibiotics were added into the monolayer cultures of HeLa cells in a 24-well plate with lumox™ fluorocarbon film bottom. Ultrasound was irradiated for 20 s with or without Bubble liposomes at 50 μg/ml. Cultures were rinsed in PBS(−) solution and examined immediately after rinsing by fluorescent microscopy (Leica Microsystems CTR4000, Wetzlar, Germany).

2.10. Statistical analysis

Data from these study were analyzed using unpaired *t*-test including Welch's correction. Results were considered to be significant when the corrected *p*-value is less than 0.05, indicated as $p < 0.05$ in the manuscript and figure legends. Error bars shown in the figures are standard deviations of duplicate samples in experiments repeated at least three times.

3. Results

3.1. Cell viability of HeLa cells and infectivity of chlamydiae by nanobubble-enhanced ultrasound

We first investigated whether nanobubble-enhanced ultrasound decreased the cell viability of HeLa cells and the infectivity of *chlamydia*. As shown in Table 1, ultrasound at intensity of 0.44 W/cm^2 caused no significant effect, but ultrasound at intensity of 0.15 W/cm^2 decreased slightly on cell viability. On the other hand, the application of ultrasound also caused no significant effect on chlamydial infectivity at both intensities of 0.15 and 0.44 W/cm^2 (Fig. 2).

Table 1
Viable cell counts following exposure of HeLa cell to ultrasound.

Application of ultrasound	Cytotoxicity: No. of viable cells/well (% of control)
Control	
(−) Sonication	7475 ± 1950
(−) Bubble liposomes	(100)
Bubble	
(−) Sonication	8940 ± 950
(+) Bubble liposomes	(120)
Ultrasound (0.15 W/cm^2)	6290 ± 950
(+) Bubble liposomes	(84)
Ultrasound (0.44 W/cm^2)	7865 ± 950
(+) Bubble liposomes	(105)

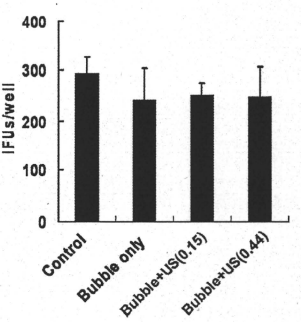

Fig. 2. Infectivity of chlamydiae by nanobubble-enhanced ultrasound. No significant change in infectivity when cells were treated with bubble liposomes (Bubble only) or ultrasound at intensities 0.15 W/cm^2 (Bubble + US(0.15)) and 0.44 W/cm^2 (Bubble + US(0.44)) in the presence of bubble liposomes.

3.2. Ultrasonic enhancement of antibiotic action on *C. trachomatis*-infected HeLa cells

The MIC of DOX for *C. trachomatis*-infected HeLa cells was determined to be 0.03 μg/ml. Infected cultures were treated with DOX at 1/2 MIC (0.015 μg/ml) then sonicated with or without the addition of Bubble liposomes (50 μg/ml). The results showed that ultrasound alone or Bubble liposomes alone did not decrease the formation of inclusions in infected cells administered with DOX (Fig. 3). However, DOX at 1/2 MIC in combination with nanobubble-enhanced ultrasound significantly reduced the number of IFUs to 66 ± 39% and 15 ± 12%, respectively, at intensities of 0.15 and 0.44 W/cm^2, compared with that administered with DOX at 1/2 MIC only (Control in Fig. 3).

The MIC of CZX for *C. trachomatis*-infected HeLa cells could not be determined because intracellular pathogens are known to be resistant to CZX, therefore, we tried to use considerably high concentrations of 0.125, 0.25, 0.5 and 1.0 μg/ml. Any of the concentrations used did not show any effect against chlamydia when applied alone but in combination with bubble-enhanced ultrasound, significant IFU reduction was observed and most with 1.0 μg/ml CZX (data not shown). Similar to the observed effect with DOX, 1.0 μg/ml CZX in combination with nanobubble-enhanced ultrasound also reduced the number of IFUs to 53 ± 32% and 50 ± 48%, respectively, at intensities of 0.15 and 0.44 W/cm^2, compared with that administered 1.0 μg/ml CZX only (Fig. 4).

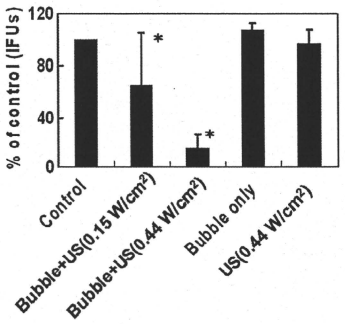

Fig. 3. Ultrasonic enhancement of bactericidal activity of doxycycline (DOX) at 1/2 MIC on *C. trachomatis*-infected HeLa cells. Data represents % of control that is the number of chlamydial inclusions treated with DOX at 1/2 MIC only (*$p < 0.05$).

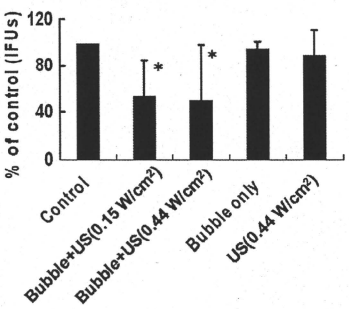

Fig. 4. Ultrasonic enhancement of bactericidal activity of ceftizoxime (CZX) at 1.0 μg/ml on *C. trachomatis*-infected HeLa cells. Data represents % of control that is the number of chlamydial inclusions treated with CZX at 1.0 μg/ml only (*$p < 0.05$).

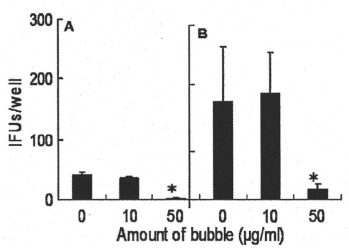

Fig. 5. Effect of concentration of Bubble liposomes in addition with ultrasound irradiation and antibiotics on *C. trachomatis*-infected HeLa cells. (A) Before ultrasound irradiation, the infected culture was treated with DOX at 1/2 MIC. (B) Before ultrasound irradiation, the infected culture was treated with CZX at 1.0 μg/ml (*$p < 0.05$).

Next, we examined the effect of the amount of Bubble liposomes on nanobubble-enhanced ultrasound reduction of IFU. With increased amount of Bubble liposomes, the synergistic effect of ultrasound and DOX was significantly increased (Fig. 5A). Bubble dose-dependent synergy was also observed with CZX and ultrasound (Fig. 5B).

3.3. Internalization of dextran–fluorescein conjugates by ultrasound

Finally, to examine whether ultrasound can facilitate intracellular uptake of large molecules, we sonicated HeLa cells in the presence of fluorescein-labeled dextran and afterwards examined the cells by fluorescence microscopy. Approximately 10% of viable cells were observed to have internalized the dextran molecules after ultrasound irradiation at intensity of 0.44 W/cm^2 in the presence of Bubble liposomes (Fig. 6). This observation showed that ultrasound can facilitate cellular uptake of large molecules.

4. Discussion

Previous reports have shown a synergistic effect between ultrasound and antibiotics in killing *E. coli* and *P. aeruginosa* [8]. The purpose of this present study was to determine if the same synergistic effect could be observed with *C. trachomatis* even if this is an intracellular organism. The results of the MIC experiments and the measurements of bactericidal activity against *C. trachomatis* show that addition of nanobubble-enhanced ultrasound to DOX treatment enhanced the effectiveness of DOX in eradicating *C. trachomatis* (Fig. 3). Dramatic reduction of IFUs to 15 ± 12% was observed at higher ultrasound intensity of 0.44 W/cm^2 (Fig. 3). These findings could have important clinical applications because the tissue concentration of antibiotics often became below the MICs in actual clinical settings.

In a previous study, the duration of the illness in patients with *C. trachomatis*-triggered reactive arthritis (ReA) was shorter in patients treated with lymecycline for 3 months than in a placebo-treated group [13]. Other studies on the long-term treatment of acute ReA with ciprofloxacin showed no advantage over placebo treatment in the outcome of ReA [14]. So far, the optimal treatment of ReA with antimicrobial drugs remains controversial. In addition, it was recently reported that persistent chlamydial infection induced ReA [15–17]. Most recent finding by Reveneau et al. have shown that persistent chlamydial forms are more resistant to DOX than acute forms because of the decreased antibiotic uptake by host cells [18]. Therefore, a more effective treatment of persistent chlamydial infections requires a method to increase antibiotics uptake by the infected cells. On the other hand, advances in ultrasound and nanobubble-enhanced ultrasound technologies have raised the possibility of using ultrasound not only for diagnostic but also for therapeutic purposes. The combination of an agent as nanobubbles and ultrasound exposure makes sonoporation possible. Sonoporation is characterized by a transient change in cellular membrane permeability mediated by ultrasound [19–24]; the cavitation energy created by the bubble collapse is thought to be the key mechanism [19]. Thereby, we confirmed that the intracellular delivery of macromolecules such as dextran was observed under the condition used in our experiments (Fig. 6). In addition, ultrasound did not damage HeLa cells or chlamydial organisms in the presence of Bubble liposomes (Fig. 2 and Table 1). This may be due to the size of the bubbles such that cavitations created are enough to deliver the drug to the cells but not "large" enough to create fatal damage to the cell itself. However, to understand the dynamic of the interactions between nanobubble, cell membrane and ultrasound [25], further study is needed. Collectively, our data suggest the possibility of using nanobubble-en-